Int. J. Multiphase Flow Vol. 9, No. 6, pp. 637–647, 1983
Printed in Great Britain.

0301–9322/83 $3.00 + .00
Pergamon/Elsevier

COUNTER CURRENT GAS–LIQUID VERTICAL FLOW, MODEL FOR FLOW PATTERN AND PRESSURE DROP

YEHUDA TAITEL and DVORA BARNEA
School of Engineering, Tel-Aviv University, Ramat-Aviv 69978, Israel

(*Received* 1 *July* 1982; *in revised form* 26 *February* 1983)

Abstract—Counter-current flow pattern transition and pressure drop are modeled. Emphasis is placed on the understanding of the transition mechanisms from a mechanistic point of view.

Unlike the case of co-current flow, in counter-current flow, the situations of "no solution" as well as "multiple solutions" for the flow pattern and pressure drop exist. These possibilities are discussed and criteria for the actual flow pattern that will take place are suggested.

Some of the results are supported by data (from the literature), others are somewhat tentative suggesting future experimental verification is needed.

INTRODUCTION

Counter-current flow has been studied primarily in connection with flooding and flow reversal as well as in connection with bubble columns.

The flooding phenomena is associated with the limit of counter-current flow; namely the limit of liquid flow rate downward under gravity caused by gas flowing upwards driven by pressure difference. Some of the most recent work on this topic are by Wallis *et al.* (1978) and Taitel *et al.* (1982) suggesting a film model to predict the flooding limit. Richter (1981) suggested that flooding occurs due to unstable wave and developed a theory for the prediction of the flooding limit. Tien *et al.* (1979) developed new correlations of the Wallis–Kutateladze type. Their derivation is based on modeling using the concept of interfacial instability coupled with kinematic wave theory and the critical wave length concept. Wallis *et al.* (1981) considered the case of flooding in many parallel vertical tubes. In spite of the progress achieved in the understanding of the flooding process (Note also the work by Shearer & Davidson 1965; Centinbudaklar & Jameson 1969; Imura *et al.* 1977; Dukler & Smith 1977; and Suzuki & Ueda 1977) it is far from being well understood and prediction techniques rely heavily on experimental correlations.

The most successful correlation is due to Wallis (1969)[1] which relates the superficial velocities of the liquid and gas at the flooding point. Of special interest is also the correlation suggested by Pushkina & Sorokin (1969) which correlates the gas flow rate at the zero liquid penetration point. Note that Pushkina and Sorokin's result is in contradiction to Wallis' (1969) correlation and it is believed (Richter 1981) that the Wallis correlation applies to small diameter pipes whereas the latter to large diameter pipes. In all the aforementioned studies, the flow pattern associated with this process is counter-current annular flow.

Counter-current flow is closely associated with bubble columns. Bubble columns are widely used as gas–liquid reactors where questions like holdup, pressure drop and interfacial area are of major importance. A thorough review of bubble columns is presented by Shah *et al.* (1978) which covers all types of gas–liquid reactors. A fairly recent work on gas holdup in bubble columns is given by Hikita *et al.* (1980). Vermeer & Kriahna (1981) considered the performance of bubble columns in the range of slug-bubble flow at superficial gas velocity above 0.1 m/s.

The performance of bubble flow can be treated by the drift flux model since, to a good approximation, the drift flux in bubble flow is a function only of the gas holdup. The classical analysis given by Wallis (1969) shows that there are three possible situations for counter-current bubble flow: (1) condition of no solution, namely the bubble column cannot operate in a steady state fashion for the liquid and gas flow rate in this region, (2) condition of two solutions, namely the bubble column can operate in two values of void fraction and (3) where only one solution exists. The latter occurs on the exact boundary between the condition of no solution and two solutions. This approach however, is valid, only in the bubble flow regime which can not exist at high void fraction (considering non-foaming systems).

In spite of the extensive work on counter-current annular flow (Flooding) and bubble flow, no work has been focused on the conditions under which either of the flow patterns exists, nor on predicting the flow pattern boundaries at which one flow pattern changes to a different one.

The flow pattern that can be observed in vertical counter-current flow are bubble flow, slug flow and annular flow. However unlike co-current flow (either upward or downward) where the flow pattern is a fairly unique function of the flow rates, multiple solutions for the flow patterns can occur in counter-current flow. Furthermore, counter-current flow may not exist for certain values of liquid and gas flow rates, again contrary to the case of co-current flow.

Figure 1 shows three cases of the typical counter-current flow patterns that may exist at the same gas and liquid flow rates. Intuitively one may realize that annular flow will exist when the bottom of the column is wide open. On the other hand bubble or slug flow will take place when the liquid valves are only slightly open. Clearly the latter is associated with much higher pressure drop owing primarily to the hydrostatic head.

The purpose of this work is to model the various flow patterns and the transition boundaries as well as the pressure drop.

MODELING

Depending on the operating conditions, i.e. gas and liquid flow rates, pipe diameter, entrance and exit conditions as well as physical properties three flow patterns may be observed: annular flow, bubble flow and slug flow.

The possible existance of each of the flow patterns is modeled and criteria for transitions from one flow pattern to another are developed. In addition the pressure drop is calculated for each flow pattern.

Annular flow

Annular flow seems to be the "most natural" flow pattern of counter current flow. It is the only flow pattern obtained for open exit lower end. The liquid is in the form of falling film for a

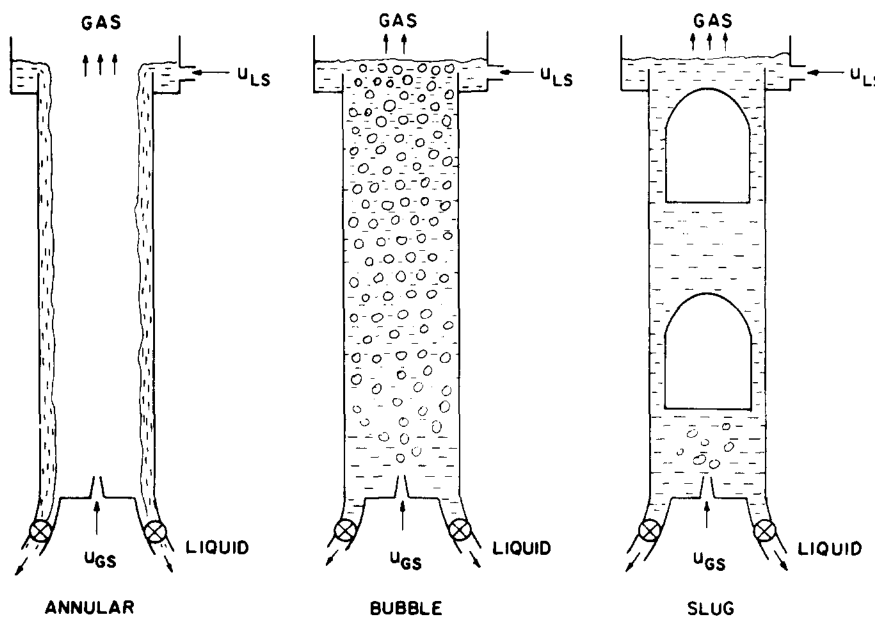

Figure 1. Flow patterns in vertical counter-current two phase flow.

wide range of gas flow rate up to the flooding point at which the downcoming liquid is swept upward. The flooding phenomenon is the limiting possible solution for counter-current flow. Thus the flooding line is the transition boundary from annular flow to "no solution". There is no acceptable theory for an accurate prediction of the flooding process. For the purpose of this study we will use Wallis correlation of the form

$$\left[\frac{u_{Gs}\rho_G^{1/2}}{\sqrt{gD(\rho_L-\rho_G)}}\right]^{1/2}+\left[\frac{u_{Ls}\rho_L^{1/2}}{\sqrt{gD(\rho_L-\rho_G)}}\right]^{1/2}=C. \quad [1]$$

In this equation u_{Gs} and u_{Ls} are the superficial velocities of the gas and liquid respectively, ρ_G and ρ_L the gas and liquid densities, g the acceleration of gravity and D the pipe diameter. C is an empirical constant of the order of unity. The transition line with $C = 1$ is shown in figure 2 for air–water at 5 cm dia. pipe by transition "a".

Since Wallis' correlation is supported by data, so is transition "a". Note however that no attempt to be very accurate was made here, and the transition line may shift somewhat if more uptodate, and possibly more accurate, correlations are used.

The pressure drop is obtained using a straightforward momentum balance on the gas core. Assuming $\delta \ll D$, no axial variations and constant properties yields:

$$\frac{dP}{dx}=-\frac{4\tau_i}{D-2\delta}-\rho_G g. \quad [2]$$

The film thickness δ is fairly constant for gas flow rates up to very close to the flooding point (Hewitt & Wallis 1963; Taitel *et al.* 1982). Thus the liquid film thickness δ can be estimated by its value for the case of free falling film. In this case (Wallis 1969) suggested that

$$\frac{\delta}{D}=K\left[\frac{\mu_L^2}{D^3g(\rho_L-\rho_G)\rho_L}\right]^{1/3}\left[\frac{\rho_L u_{Ls}D}{\mu_L}\right]^m \quad [3]$$

where μ_L is the liquid dynamic viscosity. K and m are 0.909 and 1/3 for laminar flow and 0.115 and 0.6 for turbulent flow. The film Reynolds number $(u_f\rho_L\delta/\mu_L)$ of 1000 has been shown to be the critical Reynolds number at which transition occurs.

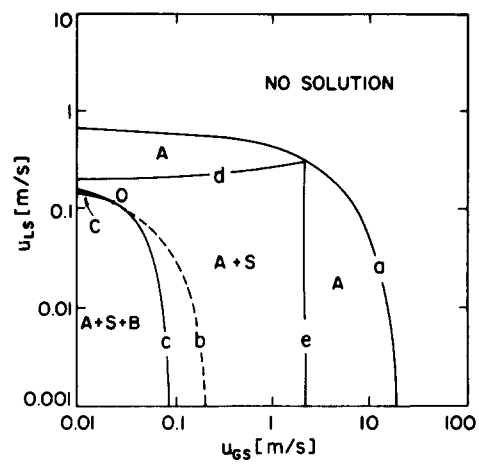

Figure 2. Flow pattern map for vertical counter-current pipes 5 cm dia., air–water at 25°C, 0.1 MPa. (A, Annular; S, slug; B, bubble).

The interfacial shears τ_i is given by

$$\tau_i = \frac{1}{2} f_i \rho_G \frac{u_{Gs}^2}{\left(1 - 2\frac{\delta}{D}\right)^4}. \qquad [4]$$

For the interfacial shear friction factor f_i Wallis correlation of the form

$$f_i = A + B\left(\frac{\delta}{D}\right)^n \qquad [5]$$

is used. Wallis suggested the values $A = 0.005$, $B = 1.5$ and $n = 1$. Admittedly the question of the interfacial shear, particularly for counter-current flow is not considered closed. Yet, Wallis' form is simple, widely used, and yields fairly satisfactory results. It should be emphasized, however that[5] is a correlation for "well behaved" concurrent annular flow, and we assume that it is also valid for "well behaved" counter current film flow. It is not valid close to the flooding point. The pressure drop variation at the exact flooding point is a complex process quite different from the "well behaved" annular film flow. It is considered in some detail by Richter (1981) and Wallis *et al.* (1981).

Bubble flow

The next flow pattern considered is bubble flow which may exist within the region bounded by "a" under certain conditions.

For counter-current bubble flow the liquid flows downwards while the gas bubble rise upwards. The relation between the liquid and gas superficial velocities and the liquid holdup ϕ is given by (Taitel *et al.* 1980)

$$u_{Ls}(1-\phi) + \phi u_{Gs} = u_0\phi(1-\phi) \qquad [6]$$

where u_0 is the relative rise velocity of the bubbles, namely $u_0 = u_L - u_G$ ($u_L = u_{Ls}/\phi$ and $u_G = u_{Gs}/(1-\phi)$). Although the rise velocity u_0 is a complex function of the bubble diameter, pipe diameter and void fraction it can be considered approximately constant for "large" bubbles and low void fraction and is given by (Harmathy 1960) correlation

$$u_0 = 1.53\left[\frac{g(\rho_L - \rho_G)\sigma}{\rho_L^2}\right]^{1/4}. \qquad [7]$$

For air–water at about 25°C and atmospheric pressure $u_0 \simeq 0.25$ m/s. Equation [6] is a quadratic equation yielding two, one or no solution for ϕ. The case of no solution is given by

$$u_{Ls} > u_{Gs} + u_0 - \sqrt{4u_{Gs}u_0}. \qquad [8]$$

This curve is shown on figure 2 by the boundary "b". Bubble flow cannot exist for liquid and gas flow rates above this line.

At $\phi < 0.7$ (void fraction greater than 0.3) bubbles tend to coallesce and form Taylor bubbles (Griffith & Synder 1964). Thus within the region of solution defined by [8] bubble flow can exist only in the subregion where $\phi > 0.7$ in [6]. The line $\phi = 0.7$ is shown in figure 2 by transition "c". As seen transition "c" is tangent to the boundary "b" at a single point 0. The region to the left of "c" corresponds to two possible solutions one of which is for $\phi > 0.7$ and the other for $\phi < 0.7$. The latter is unacceptable (for non foaming systems) and therefore this region corresponds to a single solution of bubble flow. The region to the right of "c" and left of "b", up to the point 0, is the region where both solutions yields $\phi < 0.7$ and therefore do not exist. Thus the boundary "b" to the "right" of 0 is "imaginary" and is plotted as a broken line. The small shaded region above transitions "c" and below "b" is a region where both solutions for ϕ are between 0.7 to 1. Thus, in this region two solutions of bubble flow exist. As seen, however, this region is quite small (in the range of flow rates shown in figure 2). The limiting boundary for bubble flow consists of transition "c" up to point 0 (the solid line) and transition "b" to the left of point 0.

Notice that both annular flow and bubble flow can exist for this region. The factor that will determine the actual flow pattern is the pressure drop as provided by the boundary conditions.

For very low liquid flow rate the liquid is almost stagnant and transition "c" in this region is the same as bubble-slug transition for co-current flow. Thus transition "c" in this range is supported by data that was found valid for upward co-current flow (Taitel *et al.* 1980). Note also the observation by Vermeer & Krishna (1981) for stagnant liquid systems that small bubble flow changes to "large, fast rising bubbles", namely to slug flow (for $D < 10$ cm) or Churn–Turbulent flow (for $D > 10$ cm) above $u_{G_S} \simeq 0.1$ m/s. This agrees also quite well with our proposed transition "c" at low liquid flow rate.

The pressure drop associated with bubble flow is primarily attributed to the hydrostatic head (figure 1) and depends primarily on the void fraction $\alpha = (1 - \phi)$. Thus,

$$\frac{\mathrm{d}P}{\mathrm{d}x} = -\rho_M g + \frac{2}{D} f \rho_L u_L^2 \qquad [9]$$

where the second term on the r.h.s. is the frictional pressure drop which, though small for bubble flow, can be easily taken into account. In [9] the friction factor for smooth pipes is assumed

$$f = 0.046\left(\frac{\rho_L D u_L}{\mu_L}\right)^{-0.2} \qquad [10]$$

for turbulent flow and

$$f = 16\left(\frac{\rho_L D u_L}{\mu_L}\right)^{-1} \qquad [11]$$

for laminar flow. The mixture density ρ_M is given by

$$\rho_M = \rho_L \phi + \rho_G (1 - \phi)\,. \qquad [12]$$

Note that the pressure drop is calculated on the basis of the liquid velocity. This seems to be a reasonable approach. The homogeneous model is not applicable here since we do have a slip between the phases and the homogeneous model can yield negative pressure drop (since u_M may be in the upward direction). At any rate the frictional pressure drop is so small in bubble flow that more exact methods are simply not worth the effort.

Slug flow

Bubble flow develops into slug flow beyond tranditions "c" and "b" as previously mentioned. Slug flow consists of long Taylor type bubbles separated by slugs of liquid. The term slug flow used here is an idialization of all types of intermittent flows including Churn Turbulent that has been observed in large diameter pipes. The liquid slugs may or may not contain small bubbles. For the purpose of this analysis the liquid slug will be assumed to be free of gas bubbles. The Taylor bubble has a characteristic spherical cap with a cylindrical body having a cross sectional area close to that of the pipe. The liquid confined between the bubble and the pipe flows around the bubble in the form of a falling film.

Counter current slug flow is not possible for either high liquid or high gas flow rates, where transition to annular flow must take place. Increasing liquid flow rate decreases the upward velocity of the Taylor bubbles until a limiting point is reached where gas mass balance cannot be satisfied. On the other hand increasing the gas flow rate causes flooding that limits the possible counter-current liquid flow rate. As a result, again, slug flow is not possible beyond this point.

The velocity of the Taylor bubble u_G is given quite accurately by the relation (Nicklin *et al.* 1962).

$$u_G = 1.2u_L + 0.35\sqrt{gD}. \tag{13}$$

Equation [3] was proposed for cocurrent flow, however, it has no restriction to counter current application. Continuity considerations require that

$$u_L = u_{Gs} - u_{Ls} \tag{14}$$

and

$$u_G - u_L = 4\frac{\delta}{D}(u_G + u_f) \tag{15}$$

where u_f is the film average downward velocity and δ is the film thickness.

Equation [15] is a mass balance relative to the moving gas bubble. Note also that in [15] δ/D is assumed small such that the cross sectional area of the liquid film is $\pi D\delta$. Since the liquid film adjacent to the gas bubble is in the form of a free falling film, its average velocity u_f is related to its thickness using [3] by replacing Du_{Ls} by $4u_f\delta$. The film thickness as a function of u_f is thus obtained by

$$\frac{\delta}{D} = B\left[\frac{\mu_L{}^2}{D^3g(\rho_L - \rho_G)\rho_L}\right]^p\left[\frac{4\rho_L u_f D}{\mu_L}\right]^q \tag{16}$$

where B, p and q equal to 0.00448, 5/6, 3/2 for turbulent flow and 0.8667, 1/2 and 1/2 for laminar flow respectively. The determination of laminar or turbulent flow in the film is based, as suggested by Wallis (1969), on the film Reynolds Number $Re_f = \rho_L u_f \delta/\mu_L$. Thus the film flow is turbulent for $Re_f > 1000$ and laminar for $Re_f < 1000$.

Substituting [13] and [14] in [15] yields

$$u_L = u_{Gs} - u_{Ls} = \frac{4\frac{\delta}{D}u_f - 0.35\sqrt{gD}\left(1 - 4\frac{\delta}{D}\right)}{0.2 - 4.8\frac{\delta}{D}}. \tag{17}$$

For given u_{Gs} and u_{Ls} [16] and [17] can be solved for u_f and δ/D. A convenient hand calculator explicit approach can be used by tabulating δ/D and $u_{Gs} - u_{Ls}$ as a function of u_f using [16] and [17].

The relative length of the gas bubble l_G/l can be derived from a simple mass balance on the gas that leaves the upper end of the pipe or alternatively on the liquid that leaves the bottom of the pipe assuming the gas bubble is a cylinder of constant cross sectional area. This yields

$$\frac{l_G}{l} = \frac{u_{Gs}}{4\frac{\delta}{D}u_f + (u_{Gs} - u_{Ls})}. \qquad [18]$$

For a physical solution that satisfies mass balance l_G/l should be always less than unity. Therefore

$$4\frac{\delta}{D}u_f > u_{Ls} \qquad [19]$$

limits the possibility of the slug flow pattern. The boundary [19] is plotted on figure 2 by the boundary "d" which limits the region of slug flow as liquid flow rate is increased.

A different boundary limits slug flow when gas flow rate is increased. This limit is reached when the relative velocity between the Taylor bubble and the liquid film adjacent to it reaches the condition of flooding. Equation [1] can be used for this purpose when u_{Gs} is replaced by $(1-4(\delta/D))u_G$ and u_{LS} by $4(\delta/D)u_f$. The final results using also [13] and [14] for u_G yields

$$u_{Gs} - u_{Ls} \leq \frac{\left\{C[gD(\rho_L - \rho_G)]^{1/4} - \left[4\frac{\delta}{D}u_f\rho_L^{1/2}\right]^{1/2}\right\}^2}{1.2\left(1-4\frac{\delta}{D}\right)\rho_G^{1/2}} - 0.292\sqrt{gD}. \qquad [20]$$

Thus [20] has to be satisfied for slug flow to exist. Equation [20] is plotted on figure 2 as transition "e". Notice that transitions "d", "e" and "a" intersect at a common point since at this point transition "d" represent the case when l_G/l approach unity and the slug flow approaches annular flow.

The pressure drop consists of the following contributions:

(a) The pressure drop in the liquid slug, consists of gravitational and frictional contributions

$$\left.\frac{dP}{dx}\right)_L = \left[-\rho_L g - \frac{2}{D}f_L\rho_L|u_L|u_L\right]\left(1-\frac{l_G}{l}\right). \qquad [21]$$

The friction factor f_L is calculated by [10] or [11] where u_L, the slug velocity here, is taken in its absolute value.

(b) The pressure drop in the Taylor bubble zone. It is usually very small. Still it can be easily calculated by

$$\left.\frac{dP}{dx}\right)_G = \left[-\rho_G g - \frac{4\tau_i}{D\left(1-2\frac{\delta}{D}\right)}\right]\frac{l_G}{l}. \qquad [22]$$

The second term on the r.h.s. is the frictional contribution caused by the interfacial shear τ_i. It can be calculated from

$$\tau_i = \tfrac{1}{2}f_i\rho_G\mu_G^2 \qquad [23]$$

where for f_i a correlation of the same form as [5] is used.

(c) In addition, acceleration pressure drop is associated with the mixing zone of the liquid slug at which the liquid film decelerates to the slug velocity. As in Dukler & Hubbart (1975) this pressure drop can be calculated by

$$\left.\frac{\mathrm{d}P}{\mathrm{d}x}\right)_A = \frac{(u_G - u_L)\rho_L(u_L + u_f)}{l} \qquad [24]$$

where l is the length of a slug unit. Thus unlike the previous cases where only the ratio l_G/l was needed the absolute length of a slug unit is needed here. It can be calculated on the basis of the length of the liquid slug which has been demonstrated (Taitel *et al.* 1980) to be fairly constant and equal approximately to $16D$. In this case $l = 16D/(1 - l_G/l)$.

Finally the total average pressure drop is calculated by

$$\frac{\mathrm{d}P}{\mathrm{d}x} = \left.\frac{\mathrm{d}P}{\mathrm{d}x}\right)_L + \left.\frac{\mathrm{d}P}{\mathrm{d}x}\right)_G + \left.\frac{\mathrm{d}P}{\mathrm{d}x}\right)_A . \qquad [25]$$

RESULTS AND DISCUSSION

Figure 2 shows a typical flow pattern map obtained using the aforementioned models for air–water system in 5-cm pipe at 25°C and atmospheric pressure.

Transition "a" separates the flow region into "no solution zone" and a zone where solution is possible. The region of possible solution is subdivided into 3 zones:

(1) A region "A" where only annular flow exist (above transition "d" and to the right of "e").

(2) A region "$A + S$" where only annular and slug flow can exist (left of "e", below "d" and to the right of "c").

(3) A region "$A + S + B$" where annular, slug and bubble flow can exist. This region is bounded on the right by "c" up to the point 0 and at the top, to the left of the point 0, by "b".

Note that in the small shaded area bounded by "c" and "b" two solutions for bubble flow exist. Namely two possibilities for void fraction for the same flow rates.

As seen annular flow is the dominant flow pattern which can exist in the whole range of possible solutions. It is therefore being considered here as the "most natural" flow pattern for counter current flow.

Slug flow can exist in the "$A + S$" region and the "$A + S + B$" region. Bubble flow can exist only in the "$A + S + B$" zone.

The question that arises is what determines the actual flow pattern that takes place in a zone where multiple solutions are possible:

The pressure drop associated with annular flow is about two to three orders of magnitude lower than for slug and bubble flow (accept for very high gas flow rates).

Therefore annular flow will result when low pressure exit boundary condition is imposed at the lower end of the tube. In other words when the liquid can flow with minimal restriction at the liquid exit (see figure 1). When the liquid flow is restricted the liquid will accumulate in the pipe until the static head built is sufficient to force out the liquid at a comparable rate to the annular flow pattern with no restriction. In the latter case bubble on slug flow will result.

The pressure drop in slug and bubble flow is primarily the result of the hydrostatic head. Both flow patterns have about the same order of pressure drop in the region where both patterns can exist (the "$A + S + B$" zone). As mentioned in Taitel *et al.* (1980) slug flow is unstable for pipes where the free rise velocity of a Taylor bubble in slug flow exceed the rise velocity of the bubbles. Namely when

$$0.35\sqrt{gD} > 1.53\left[\frac{g(\rho_L - \rho_G)\sigma}{\rho_L^2}\right]^{1/4} . \qquad [26]$$

The mechanistic explanation is as follows: Slug flow is generated through spontaneous agglomeration of bubbles. In slug flow, however, bubbles are torn away from the back end of the Taylor bubble owing to the vigorous mixing of the free falling film that penetrates the liquid slug. If the bubbles move slower than the Taylor bubble they are left behind and eventually the slug flow pattern is destroyed, maintaining the bubble flow pattern. Thus the region "$A+S+B$" will result in bubble flow in large diameter pipes and slug flow in small diameter pipes. For air–water this occurs at pipe diameter of about 5 cm. In spite of the aforementioned, bubble flow can exist also in small diameter pipe if special efforts are taken to introduce the bubbles at a small diameter. Bubbles of small size tend to behave as rigid spheres and resist agglomeration and therefore can exist also in small diameter pipes. Thus it is estimated that when the bubble diameter is less than (Brodkey 1967),

$$d < \left[\frac{0.4\sigma}{(\rho_L - \rho_G)g}\right]^{1/2} \quad [27]$$

the bubbles will not coalesce to form slugs.

The results for pressure drop are shown in figure 3 for air–water system. The variation of the pressure drop with the gas flow rate u_{Gs} is plotted for 3 different liquid flow rates. The curves are terminated at the boundary beyond which the particular flow pattern cannot exist.

As seen the pressure drop associated with annular flow is two to three folds lower than for the case of bubble and slug flow. This of course is a direct result of the high void fraction associated with annular flow. For bubble and slug flow the major contribution to the pressure drop results from the gravitational head which approaches that of the liquid at low gas flow rate.

It is interesting to observe that the pressure drop increases with gas flow rate for annular flow while it decreases for bubble and slug flow. This, of course, is owing to the increase in void fraction with increasing u_{Gs} for bubble and slug flow while in annular flow the void fraction remains the same (more accurately it decreases a little near the flooding point) and the pressure drop is primarily due to interfacial shear.

Furthermore, for slug and bubble flow the pressure decreases with increasing liquid flow rate contrary to annular flow and also contrary to slug and bubble flow in co-current upward gas liquid flow. This is the result of the increase in the gas holdup caused by increasing the liquid downward velocity which decreases the absolute upward velocity of the bubbles.

SUMMARY AND CONCLUSIONS

Models for predicting flow pattern transition boundaries and pressure drop for counter-current vertical flow are developed.

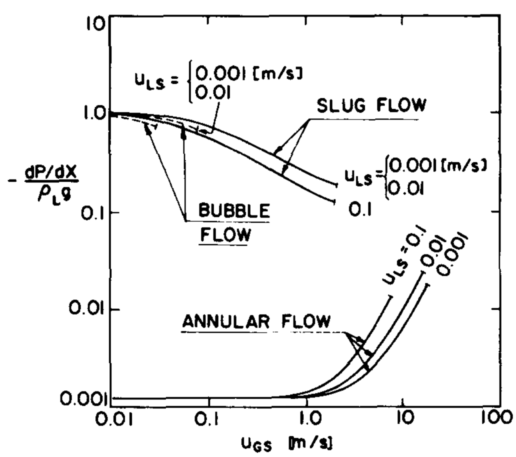

Figure 3. Pressure drop for vertical counter-current pipes, 5 cm dia., air–water at 25°C, 0.1 MPa.

Transition "a" is the result of flooding in annular flow beyond which no possible solution can exist. Transition "b" and "c" limit bubble flow. The former to the region where bubble flow can exist while the latter to the region where the void fraction is less than 0.3. Thus the bubble flow pattern is bounded by a section of transition "c" (at lower liquid flow rate) and a section of transition "b".

Transition "d" and "e" limit the region of slug flow. Transition "d" is caused by the inability of flow rates above "d" to satisfies mass balance for slug flow. Transition "e" is caused by reaching flooding condition.

The question of multiple solution for the flow pattern can be summarized as follows:

(1) Annular flow can exist in the whole range and will take place in the case where the liquid outlet is not restricted (open exit).

(2) Bubble flow will take place in the "$A + S + B$" zone in pipes of large diameter as given by [26]. Also bubble flow will take place if the bubbles, introduced into the column are very small [27].

The aforementioned theory is based on a mechanistic approach that put together known experimental observations and correlations in order to construct a complete picture of the flow pattern map. The accuracy of the approach depends on the correlations used. However, as has been demonstrated so many times in the past, accuracy in flow pattern transitions is impossible and usually not necessary.

Experimental evidence is provided to confirm the validity of some of the transition lines. This applies to transition "a" and "c" (at low liquid flow rate). More experimental work is needed to verify the complete theory.

The calculation for the pressure drop are based on acceptable correlations for the friction factor at the wall and the interface. The correlation for the friction factor [5] however does not apply very close to the flooding point. Therefore, the results for the pressure drop are likely to be wrong near transition "e" and "a".

REFERENCES

Brodkey, R. S. 1967 *The Phenomena of Fluid Motions*. Addison-Wesley, Reading, Mass.

Centinbudaklar, A. G. & Jameson, G. J. 1969 The mechanism of flooding in vertical counter current two-phase flow. *J. Fluid Mech.* **22**, 1669–1680.

Dukler, A. E. & Hubbard, M. G. 1975 A model for gas–liquid slug flow in horizontal and near horizontal tubes. *I&EC Fund.* **14**, 337–347.

Dukler, A. E. & Smith, L. 1977 Two-phase interactions in counter-current flow studies of the flooding mechanism. U.S. Nuclear Regulatory Agency Rep. NUREG/CR-0617.

Griffith, P. & Synder, G. A. 1964 The bubbly-slug transition in a high velocity two-phase flow. MIT Rep. 5003-29 (TID-20947).

Harmathy, T. Z. 1960 Velocity of large drops and bubbles in media of infinite or restricted extent. *AIChE J.* **6**, 281–288.

Hewitt, G. F. & Wallis, G. B. Nov. 17–22 1963 Flooding and associated phenomena in falling film flow in a tube. *Proc. ASME Multi-Phase Symp.* Philadelphia, p. 62.

Hikita, H., Asai, S., Tanigawa, K., Segawa, K. & Kitao, M. 1980 Gas hold-up in bubble columns. *Chem. Engng J.* **20**, 59–67.

Imura, H., Kusuda, H. & Funatsu, S. 1977 Flooding velocity in a counter-current annular two-phase flow. *Chem. Engng Sci.* **32**, 79–87.

Nicklin, D. J., Wilkes, J. O. & Davidson, J. F. 1962 Two phase flow in vertical tubes. *Trans. Inst. Chem. Engrs (Lond.)* **40**, 61–67.

Pushkina, O. L. & Sorokin, Y. L. 1969 Breakdown of liquid film motion in vertical tubes. *Heat Transf. Soviet Res.* **1**, 56–64.

Richter, H. J. 1981 Flooding in tubes and annuli. *Int. J. Multiphase Flow* **7**, 647–658.

Shah, Y. T., Stiegel, G. J. & Sharma, M. M. 1978 Backmixing in gas–liquid reactors. *AIChE J.* **24**, 369–400.

Shearer, C. J. & Davidson, J. F. 1965 The investigation of a standing wave due to gas blowing upwards over a liquid film; its relation to flooding in wetted wall columns. *J. Fluid Mech.* **22**, 321–335.

SUZUKI, S. & UEDA, T. 1977 Behavior of liquid films and flooding in counter-current two-phase flow—I. Flow in circular tubes. *Int. J. Multiphase Flow* **3**, 517–532.

TAITEL, Y., BARNEA, D. & DUKLER, A. E. 1980 Modelling flow pattern transition for steady upward gas–liquid flow in vertical tubes. *AIChE J.* **26**, 345–354.

TAITEL, Y., BARNEA, D. & DUKLER, A. E. 1982 A film model for the prediction of flooding and flow reversal for gas–liquid flow in the vertical tubes. *Int. J. Multiphase Flow* **8**, 1–10.

TIEN, C. L., CHUNG, K. S. & LIU, P. C. 1979 Flooding in two-phase countercurrent flows. EPRI Rep. NP-1283.

VERMEER, D. J. & KRISHNA, R. 1981 Hydrodynamics and mass transfer in bubble columns operating in the churn-turbulent regime. *I&EC Process Design & Devel.* **20**, 475–482.

WALLIS, G. B., RICHTER, H. J. & BHARATHAN, D. 1978 Air–water counter-current annular flow in vertical tubes. EPRI Rep. NP-786.

WALLIS, G. B. 1969 *One Dimensional Two-Phase Flow.* McGraw-Hill, New York.

WALLIS, G. B., KARLIN, A. S., CLARK, III, C. R., BHARATHAN, D., HAGI, V. & RICHTER, H. J. 1981 Countercurrent gas–liquid flow in parallel vertical tubes. *Int. J. Multiphase Flow* **7**, 1–19.